CDF note 10778

Measurement of the B_s^0 Mixing Phase using $B_s^0 \to J/\psi\phi$ Decays from the Full Run II Dataset

The CDF Collaboration
URL `http://www-cdf.fnal.gov`
(Dated: April 18, 2012)

We report an update of the measurement of the *CP*–violating B_s^0 mixing phase $\beta_s^{J/\psi\phi}$ in flavor–tagged $B_s^0 \to J/\psi\phi$ decays using the full CDF Run II dataset and corresponding to an integrated luminosity of about $9.6\,\mathrm{fb}^{-1}$. We reconstruct approximately 11 000 $B_s^0 \to J/\psi\phi$ decays, thus almost doubling the event sample size over the previous iteration of the analysis, and report confidence regions in one– and two-dimensional $\beta_s^{J/\psi\phi}$ and $(\beta_s^{J/\psi\phi}, \Delta\Gamma_s)$ spaces. We find $\beta_s^{J/\psi\phi} \in [-\pi/2, -1.51] \bigcup [-0.06, 0.30] \bigcup [1.26, \pi/2]$ at the 68% confidence level. By restricting to the solution corresponding to a positive value for the decay width difference the value of the mixing phase agrees with the expectation from the CKM hierarchy. Assuming the SM value for $\beta_s^{J/\psi\phi}$, we also measure the mean B_s^0 lifetime, the decay-width difference between the heavy and light B_s^0 mass eigenstates, the decay transversity amplitudes and strong phase to be

$$\begin{aligned}
\tau(B_s^0) &= 1.528 \pm 0.019\ (\mathrm{stat}) \pm 0.009\ (\mathrm{syst})\,\mathrm{ps}, \\
\Delta\Gamma_s &= 0.068 \pm 0.026\ (\mathrm{stat}) \pm 0.007\ (\mathrm{syst})\,\mathrm{ps}^{-1}, \\
|A_0(0)|^2 &= 0.512 \pm 0.012\ (\mathrm{stat}) \pm 0.017\ (\mathrm{syst}), \\
|A_\parallel(0)|^2 &= 0.229 \pm 0.010\ (\mathrm{stat}) \pm 0.014\ (\mathrm{syst}), \\
\delta_\perp &= 2.79 \pm 0.53\ (\mathrm{stat}) \pm 0.15\ (\mathrm{syst})\,\mathrm{rad}.
\end{aligned}$$

All results are consistent with determinations from other experiments. They also agree and supersede previous CDF determinations.

Preliminary Results for Winter 2012 Conferences

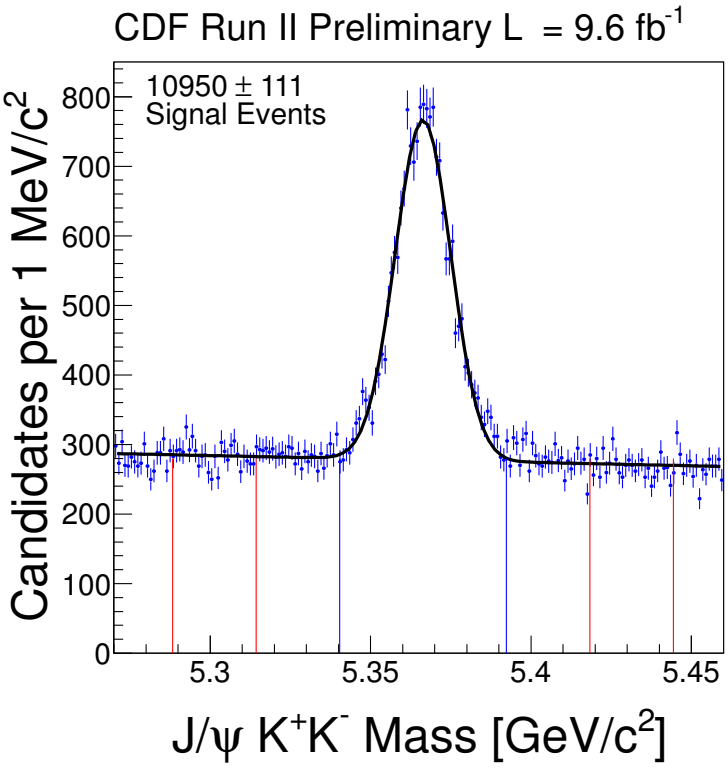

Figure 1. Mass distribution of our final dataset. Blue lines show the signal region, and red lines the sidebands.

I. INTRODUCTION

The understanding of *CP* violation in the B_s^0 sector is far from being established and still offers room for possible non-SM contributions, as possibly indicated by the anomaly in the dimuon charge asymmetry reported by the D0 Collaboration [2]. We present an update on the full Run II dataset of the measurement of the *CP*–violating phase $\beta_s^{J/\psi\phi}$ in $B_s^0 \to J/\psi(\to \mu^+\mu^-)\phi(\to K^+K^-)$ decays. The previous CDF measurement, based on $5.2\,\mathrm{fb}^{-1}$ of data, is in agreement with the prediction from the CKM hierarchy [1]. The present measurement follows closely the techniques and strategy of the previous tagged analysis [1] and is based on the full dataset collected by the CDF di-muon trigger between February 2002 and September 2011. The reconstructed signal candidates are selected via an artificial neural network (ANN). A fit to their time-evolution that uses information on production flavor, mass, decay time, and decay angles determines the observables of interest. The only major difference with respect to the previous iteration of the analysis is the use of an updated calibration for the Opposite-Side-Tagging algorithm. The information from the Same-Side-Kaon-Tagging is instead restricted to only half of the sample.

II. DATA SELECTION AND RECONSTRUCTION

The reconstruction begins with searching for J/ψ candidates by kinematically fitting to a common vertex the two oppositely-charged muon candidates that fired the online di-muon trigger [3]. All pairs of oppositely-curved tracks in the event (except the di-muons) are then fitted to a common vertex with kaon mass hypothesis for each. If their kinematics is consistent with a ϕ meson decay, the four tracks are combined in a kinematic fit to a common three-dimensional decay point, constraining also the di-muon mass to the known J/ψ mass [4]. The surviving events are then subjected to a loose initial selection to suppress background followed by an ANN selection, both of which are described in [1]. The selection criteria have been optimized so as to minimize the expected average uncertainty on the $\beta_s^{J/\psi\phi}$ measurement, as estimated by large ensembles of statistical trials.

Fig. 1. shows the resulting $J/\psi K^+K^-$ mass distribution. A prominent $B_s^0 \to J/\psi\phi$ signal containing approximately 11 000 decays, centered at the nominal B_s^0 mass and about $9\,\mathrm{MeV}/c^2$ wide, emerges from a smooth, approximately uniformly distributed, background. The background is nearly saturated by the combinatorial component, which is

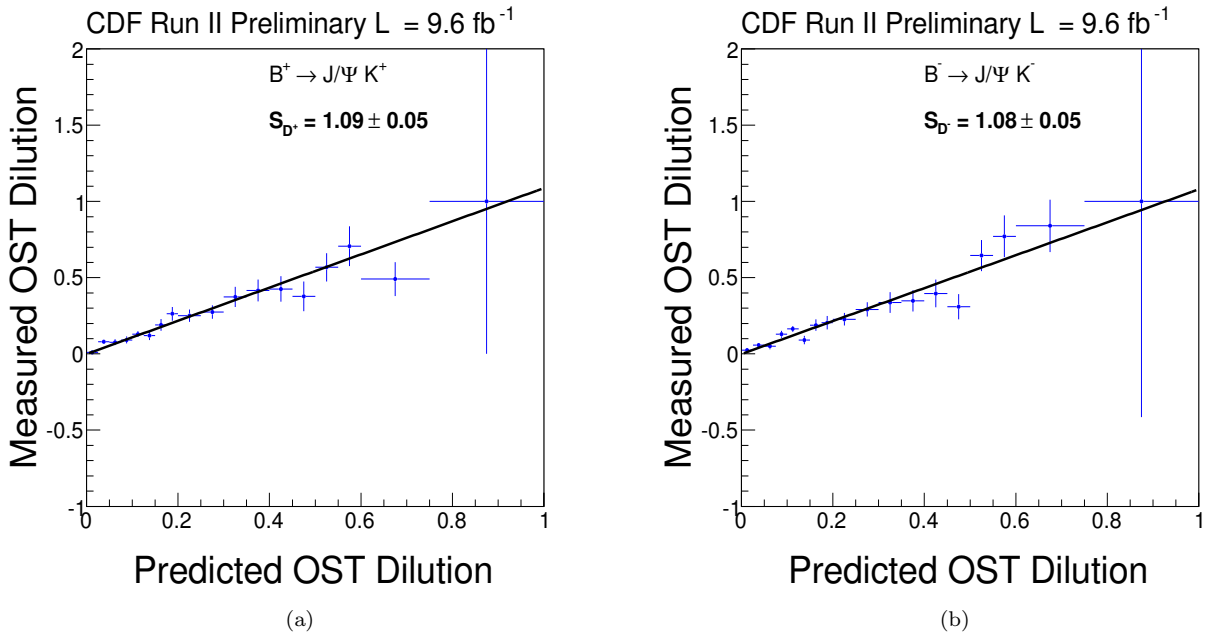

(a) (b)

Figure 2. Measured dilution as a function of predicted dilution for sideband-subtracted $B^+ \to J/\psi K^+$ (a) and $B^- \to J/\psi K^-$ (b) decays.

mainly promptly-produced and dominated by accidental combinations of two charged tracks with a real J/ψ decay. A small contribution from $B^0 \to J/\psi K^*$ decays, where the $K\pi$ pair from the K^* decay is mis-reconstructed as a ϕ decay (B^0 cross-feed) is known to contribute predominantly in the higher mass side of the signal. This contamination is not included in the default likelihood fit, and a systematic uncertainty is associated. Scalar non-resonant $B^0 \to J/\psi K\pi$ contributions are neglected. Additional contributions from S-wave K^+K^- in the ϕ signal region can originate from B_s^0 decays into $J/\psi f_0(980)$ and non-resonant $J/\psi KK$ final states giving non-negligible contributions to the B_s^0 signal. These is properly accounted in the angular portion of the fit to avoid biases in the determination of physics observables.

III. FLAVOR TAGGING

Flavor tagging algorithms are of crucial importance in enhancing the sensitivity to the CP–violating phase $\beta_s^{J/\psi\phi}$. They exploit the properties of b quark hadronization and decay to infer the flavor content (b quark or $\bar{b}$ quark) of the bottom strange meson at production. Two classes of flavor tagging algorithms are used, SSKT and OST. The SSKT algorithms deduce the production flavor of the signal bottom meson by exploiting charge-flavor correlations of the neighboring particles (kaons in the case of bottom strange mesons) produced during its fragmentation. The OST algorithms exploit pair $p\bar{p} \to b\bar{b}$ production using information from the decay of the "opposite side" bottom hadron in the event and assuming that it was not a neutral meson which undergoes oscillation.

The tagging algorithms output a tag decision indicating whether the meson was B_s^0 or $\overline{B}_s^0$ at the time of production, as well as a dilution factor $\mathcal{D}$. The dilution quantifies the mistagging rate as $\mathcal{D} = (N_R - N_W)/(N_R + N_W)$, where N_R (N_W) is the number of correctly (wrongly) tagged events.

A. Opposite Side Tagger

Different OST algorithms have been developed in CDF, using semi–leptonic decays, and jet or opposite–side kaon charge. An ANN combination of them has been validated and used in the previous measurement of the B_s^0 mixing phase. In this update, we use the same approach, after updating the extraction of the scale factors to the full Run II dataset. This is achieved by applying the OST algorithms to a sample of approximately 81 000 fully reconstructed $B^+ \to J/\psi K^+$ decays. The tagging decision and the associated dilution are then compared to the actual b quark content of the meson at production time, which is known from the charge of the kaon, since charged B do not oscillate.

Distributions of background-subtracted measured versus predicted dilutions are fit to a straight line to determine a dilution scale factor $S_{\mathcal{D}}$, as shown in Fig. 2. We determine two scale factors, one for the B^+ and one for the B^-, in order to allow for any asymmetry in the OST algorithm. We find $S_{\mathcal{D}}^+ = 1.09 \pm 0.05$ and $S_{\mathcal{D}}^- = 1.08 \pm 0.05$ respectively with a total average dilution of $\langle \mathcal{D} \rangle = 6.88 \pm 0.03\%$ and a tagging efficiency of $92.8 \pm 0.1\%$. Since the calibrated values of the scale factor for the B^+ and B^- are approximately equal we use the average value, $S_{\mathcal{D}} = 1.09 \pm 0.04$, in the fit and the spread as a systematic uncertainty.

B. Same Side Kaon Tagger

The SSKT used in this analysis was originally developed for the B_s^0 mixing measurement and is calibrated on $5.2\,\mathrm{fb}^{-1}$ of data by repeating such measurement and extracting the dilution [5]. We have not yet extended the calibration of the SSKT to the full Run II dataset. Hence, we choose not to use the information from this tagger in the second half of the data. This conservative choice prevents potential problems arising from drift of the tagger performances as a function of time and has a limited impact on the final measurement. We estimated, using simulated experiments, that the average improvement in $\beta_s^{J/\psi\phi}$ resolution when including the SSKT in the full sample with a dilution known to the same level of accuracy as for the first $5.2\,\mathrm{fb}^{-1}$ dataset does not exceed 12%.

IV. UNBINNED MAXIMUM LIKELIHOOD FIT

An unbinned maximum likelihood fit to the data is used to extract the parameters of interest, $\beta_s^{J/\psi\phi}$ and $\Delta\Gamma_s$, plus additional parameters (referred to as "nuisance parameters") that include the signal fraction and mass of the B_s^0 meson, the mean B_s^0 lifetime $\tau(B_s^0)$ and background lifetime parameters, the mixing frequency Δm_s and the flavor–tagging efficiencies and scale factors, the magnitudes of the polarization amplitudes, $|A_0|^2$, $|A_\parallel|^2$ and $|A_\perp|^2 \equiv 1 - |A_0|^2 - |A_\parallel|^2$, and angular background parameters, and the strong phases $\delta_\parallel = \arg(A_0^* A_\parallel)$ and $\delta_\perp = \arg(A_0 * A_\perp)$. The fit observables are the reconstructed $J/\psi K^+K^-$ mass m and its uncertainty σ_m, the B_s^0 candidate proper decay time t and its uncertainty σ_{ct}, the transversity angles $\cos\vartheta_T$, ϕ_T, and $\cos\psi_T$, and the flavor–tagging information $\mathcal{D}_p$ and ξ, where $\mathcal{D}$ is the event-specific dilution and $\xi = \{-1, 0, +1\}$ is the tag decision, in which $+1$ corresponds to a candidate tagged as B_s^0, -1 to a $\overline{B}_s^0$ and 0 to an untagged candidate. In our fit we also consider a possible S–wave component so the fit also measure its fraction f_{SW} and its relative phase δ_{SW}.

The full likelihood function can be expressed for signal (s) and background (b) events as

$$\mathcal{L} = \prod_{i=1}^{N} \big[f_s \cdot P_s(m|\sigma_m) \cdot P_s(\xi) \cdot P_s(\vartheta_T, \phi_T, \psi_T, ct|\sigma_{ct}, \xi, \mathcal{D}_p) \cdot P_s(\sigma_{ct}) \cdot P_s(\mathcal{D}_p) \\ + (1 - f_s) \cdot P_b(m) \cdot P_b(\xi) \cdot P_b(ct|\sigma_{ct}) \cdot P_b(\vartheta_T) \cdot P_b(\phi_T) \cdot P_b(\psi_T) \cdot P_b(\sigma_{ct}) \cdot P_b(\mathcal{D}_p) \big],$$

where the product runs over all N events in the data sample and f_s and $(1 - f_s)$ are the fraction of signal and background events, respectively. The implementation of the single probability distribution functions (PDFs) is the same to that used previously [1] with the only exception that for the new data only the OST tagging information is used.

A. Measurement of the Mixing Phase

The fit projections for the proper decay time, either assuming the SM value for the mixing phase or not, are shown in Figs. 3 and 4. Projections for the transversity angles $\cos\vartheta_T$, ϕ_T, and $\cos\psi_T$ are shown in Figs. 5 and 6. The likelihood provides a satisfactory modeling of the data

Before fitting the data, we performed extensive tests of the fitting procedure using statistical trials. We observe that, even with the current statistics, the maximum likelihood estimate is biased for the parameters of interest, and the bias can be dependent on the true values of the physics observables that are measured. Rather than quoting point estimates we use the profile-likelihood ratio ($-2\Delta\log\mathcal{L}$) as a χ^2 variable to derive to determine confidence level (CL) regions in the $\beta_s^{J/\psi\phi}$ and $(\beta_s^{J/\psi\phi}, \Delta\Gamma_s)$ spaces. However, simulations show that the observed profile-likelihood ratio deviates from a true χ^2 distribution. In particular, the resulting confidence regions contain true values of the parameters of interest with lower probability than the nominal CL. In addition, the profile-likelihood ratio appears to depend on the true values of the nuisance parameters, which are unknown. We use a large number of pseudoexperiments to

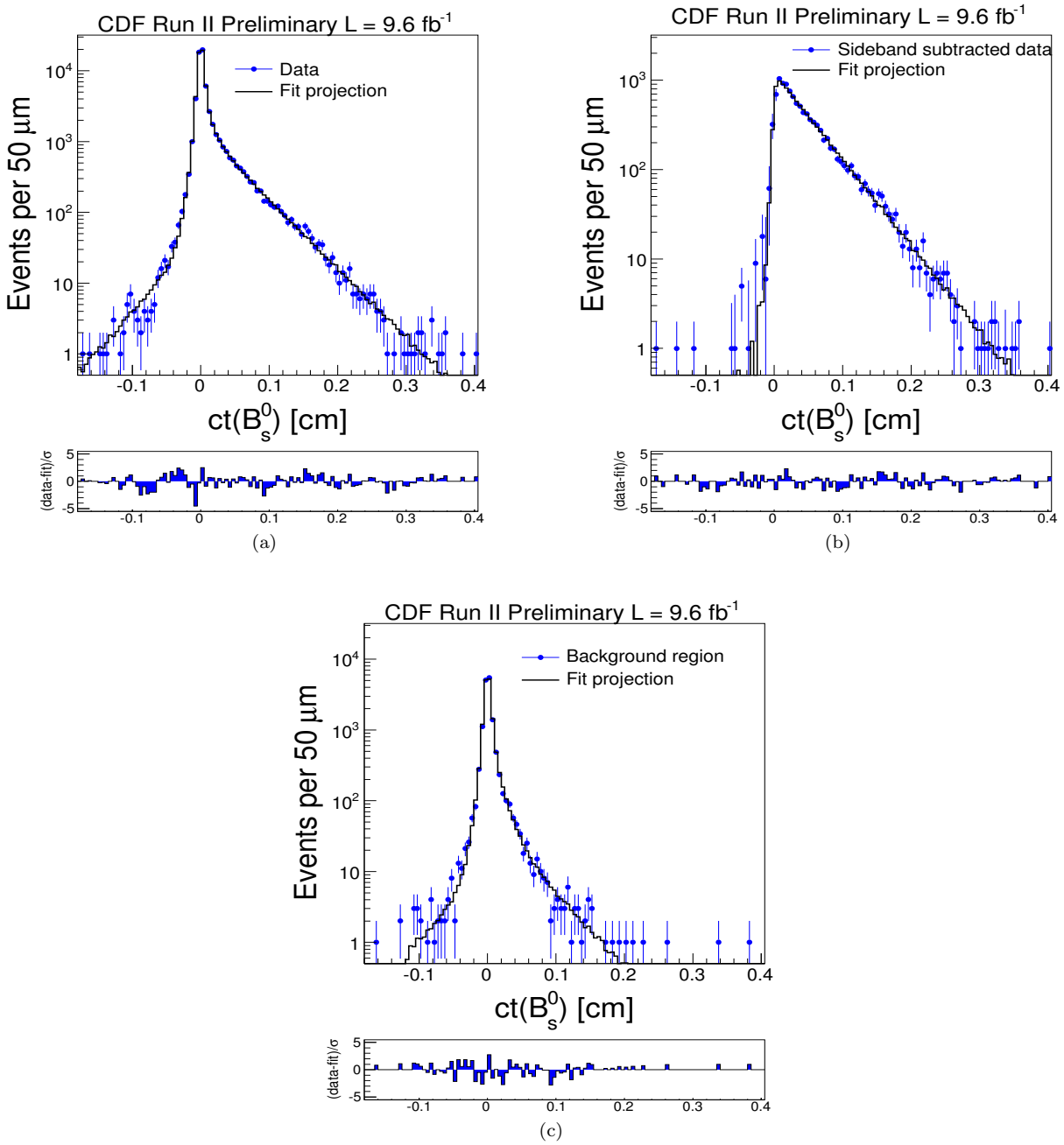

Figure 3. Proper decay time fit projections for all candidates (a), for sideband-subtracted signal (b), for candidates in the sideband regions (c). The pull distributions at the bottom show the difference between data and fit value normalized to the data uncertainty. These projections refer to the full fit with $\beta_s^{J/\psi\phi}$ floating.

derive the actual profile-likelihood ratio distribution relevant for our data. The effect of systematic uncertainties is accounted for by randomly sampling a limited number of points in the space of all nuisance parameters and using the most conservative of the resulting profile-likelihood ratio distributions to calculate the final confidence region. The coverage adjustment procedure is described in detail in Ref. [1].

The solid black histogram in Fig. 7(a) shows the profile-likelihood ratio distribution for our measurement as estimated by pseudoexperiments, compared to the ideal χ^2 curve. The colored, dashed distributions corresponds to alternate profile-likelihood ratio distributions corresponding to different arbitrary values of the nuisance parameters. We use the p-value of the most conservative ensemble to determine the corresponding 68% and 95% confidence regions for our data. This procedure is called "coverage adjustment" since it enforces that the resulting confidence intervals

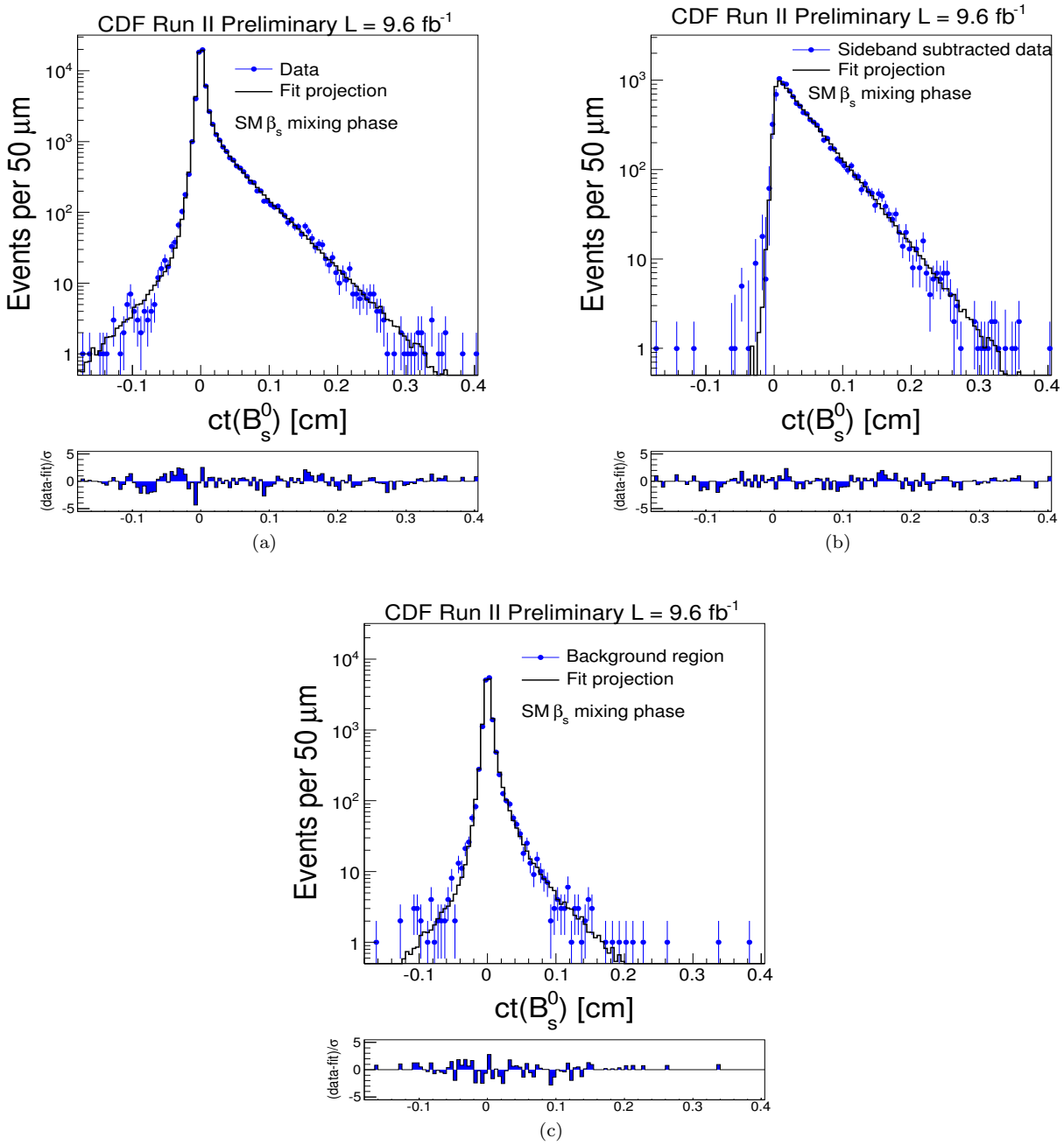

Figure 4. Proper decay time fit projections for all candidates (a), for sideband-subtracted signal (b), and for candidates in the sideband regions (c). The pull distributions at the bottom show the difference between data and fit value normalized to the data uncertainty. These projections refer to the fit with $\beta_s^{J/\psi\phi}$ fixed at the value expected from the CKM hierarchy.

have statistical coverage close to nominal.

A similar coverage adjustment procedure is carried out to determine a one-dimensional confidence interval for $\beta_s^{J/\psi\phi}$. When determining the $\beta_s^{J/\psi\phi}$ confidence interval, $\Delta\Gamma_s$ is randomized in the pseudoexperiment generation and treated as any other nuisance parameter. Fig. 8(a) shows the profile-likelihood ratio distribution observed in pseudo experiments mimicking our data. The interval $\beta_s^{J/\psi\phi} \in [-\pi/2, -1.51] \bigcup [-0.06, 0.30] \bigcup [1.26, \pi/2]$ ($[-\pi/2, -1.36] \bigcup [-0.21, 0.53] \bigcup [1.04, \pi/2]$) contains the true value of $\beta_s^{J/\psi\phi}$ at the 68% (95%) CL, as shown from the profile-likelihood scan of Fig. 8(b).

Assuming the SM CKM hierarchy, the probability to observe a mixing phase as in our data or larger is p-value =

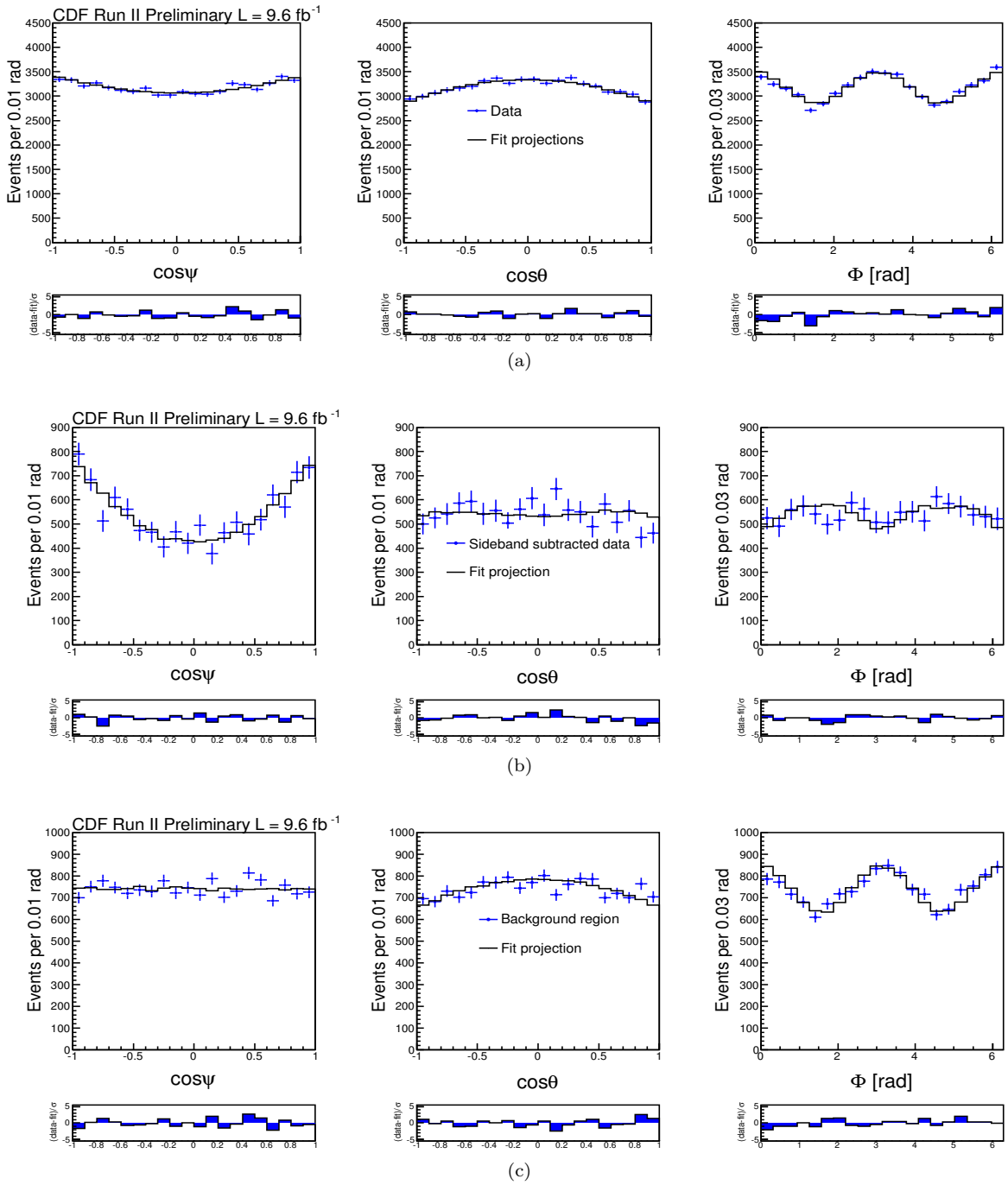

Figure 5. Transversity angles fit projections for all candidates (a), for the sideband-subtracted signal (b), and for candidates in the sideband region (c). The pull distributions at the bottom show the difference between data and fit value normalized to the data uncertainty. These projections refer to the full fit with $\beta_s^{J/\psi\phi}$ floating.

0.54 as is also evidenced in Figs. 7(b) and 8(b). The result nicely compares with most recent measurements of $\beta_s^{J/\psi\phi}$ from the D0 [6] and LHCb [7] Collaborations.

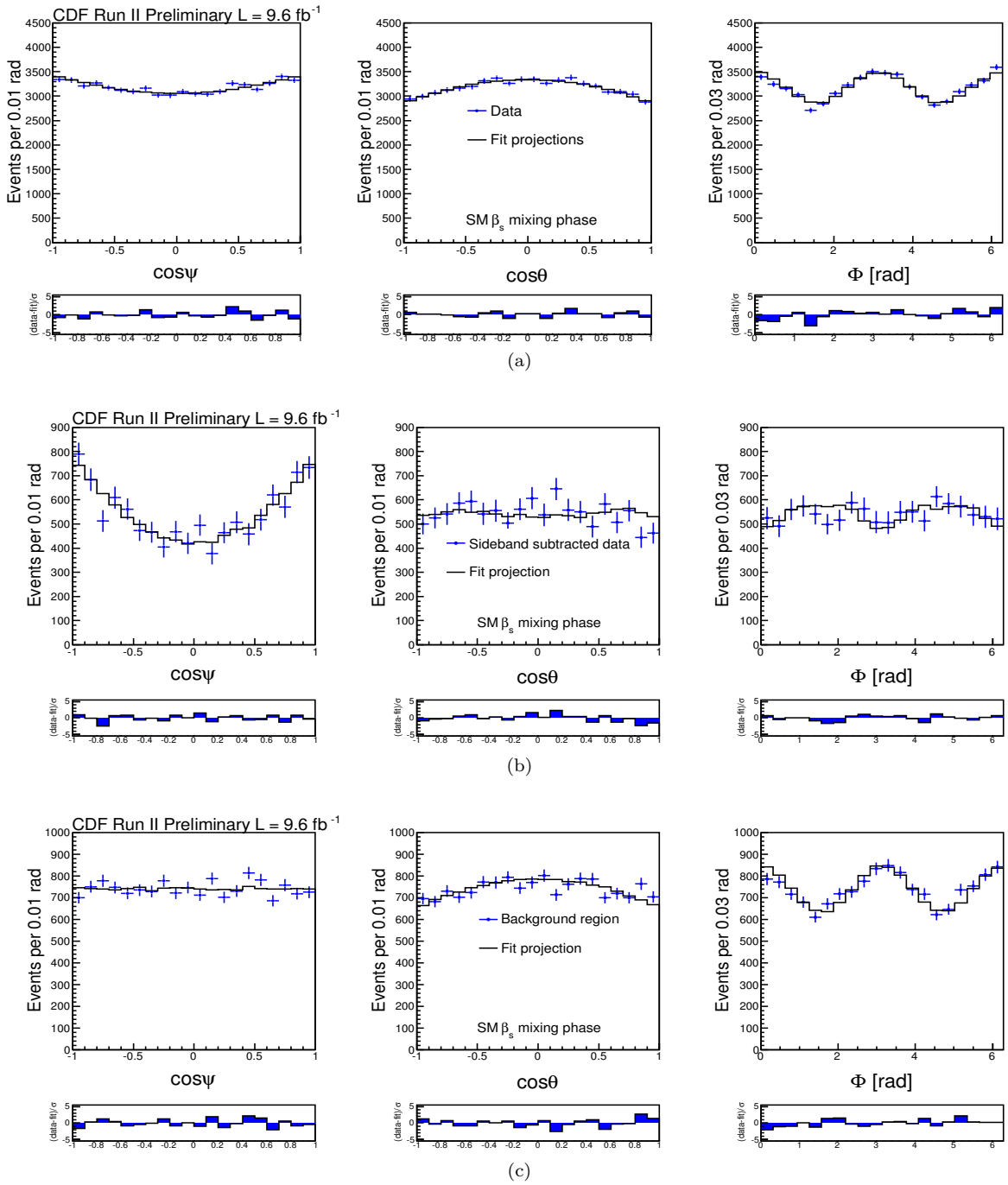

Figure 6. Transversity angles fit projections for all candidates (a), for the sideband-subtracted signal (b), and for candidates in the sideband region (c). The pull distributions at the bottom show the difference between data and fit value normalized to the data uncertainty. These projections refer to the fit with $\beta_s^{J/\psi\phi}$ fixed to the value expected from the CKM hierarchy.

B. Results under the assumption of a SM value for the mixing phase

The likelihood function in which the *CP*–violation parameter $\beta_s^{J/\psi\phi}$ is fixed to a value very close to zero ($\beta_s^{J/\psi\phi} = 0.02$), returns un-biased results for the mean B_s^0 lifetime $\tau(B_s^0)$, the decay width difference $\Delta\Gamma$, the polarization fractions $|A_{\|}(0)|^2$ and $|A_0(0)|^2$ as well as the strong phase $\delta_{\perp}$. We also observe that the likelihood function is

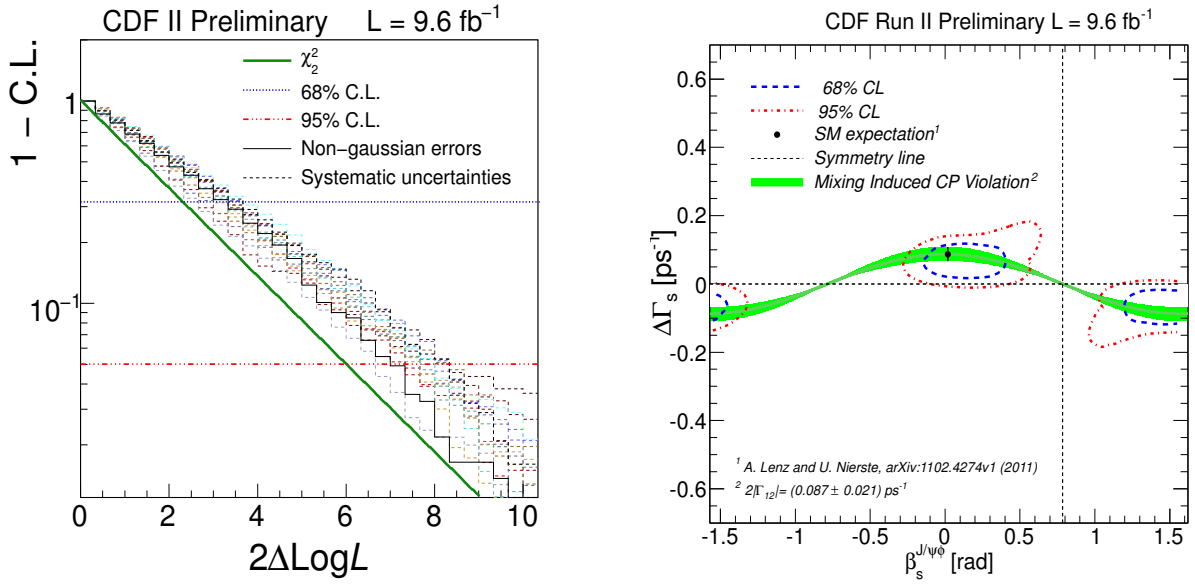

(a) (b)

Figure 7. Profile-likelihood ratio distribution with two degrees of freedom ($\beta_s^{J/\psi\phi}$, $\Delta\Gamma_s$) observed in pseudoexperiments mimicking our data (a) and corresponding confidence regions (b) in the ($\beta_s^{J/\psi\phi}, \Delta\Gamma_s$) plane. The 2D Likelihood contours have been updated since the Winter 2012 conferences, using a finer binning and excluding failed fits from the computation of the profile-likelihood ratios.

Gaussian. Hence, we provide measurements for the following quantities:

$$\begin{aligned}
\tau(B_s^0) &= 1.528 \pm 0.019\ (\text{stat}) \pm 0.009\ (\text{syst})\ \text{ps}, \\
\Delta\Gamma_s &= 0.068 \pm 0.026\ (\text{stat}) \pm 0.007\ (\text{syst})\ \text{ps}^{-1}, \\
|A_0(0)|^2 &= 0.512 \pm 0.012\ (\text{stat}) \pm 0.014\ (\text{syst}), \\
|A_\parallel(0)|^2 &= 0.229 \pm 0.010\ (\text{stat}) \pm 0.017\ (\text{syst}), \\
\delta_\perp &= 2.79 \pm 0.53\ (\text{stat}) \pm 0.15\ (\text{syst})\ \text{rad}.
\end{aligned} \tag{1}$$

We do not quote a result for $\delta_\parallel$ since the estimate of this parameter is approximately at the boundary ($\approx \pi$) resulting in a irregular likelihood shape around the minimum. The correlation matrix for the main physical parameters of the fit is presented in Table I.

	$\Delta\Gamma_s$	$\alpha_\perp$	$\alpha_\parallel$	$\delta_\perp$
$\tau(B_s^0)$	0.52	-0.16	0.07	0.03
$\Delta\Gamma_s$		-0.17	0.06	-0.01
$\alpha_\perp$			-0.53	-0.01
$\alpha_\parallel$				0.05

Table I. Correlation coefficients between physical parameters as estimated by the fit with $\beta_s^{J/\psi\phi}$ fixed to its SM value.

Systematic uncertainties are assigned for several effects that are not accounted for in the likelihood fit. Such effects include potential mis-parameterization in the fit model, impact of particular assumptions in the fit model, and physical effects which are not well known or fully incorporated into the model. In most cases, systematic uncertainties are evaluated by comparing fit results from ensembles of pseudoexperiments generated with the default model and with a model varied according to the systematic effect being investigated. Cross checks obtained by repeating the fit on real data with the modified likelihood give consistent results. The systematic uncertainty deriving from imperfect knowledge of the vertex detector alignment is assumed to be 2 μm for the lifetime, as established in previous CDF

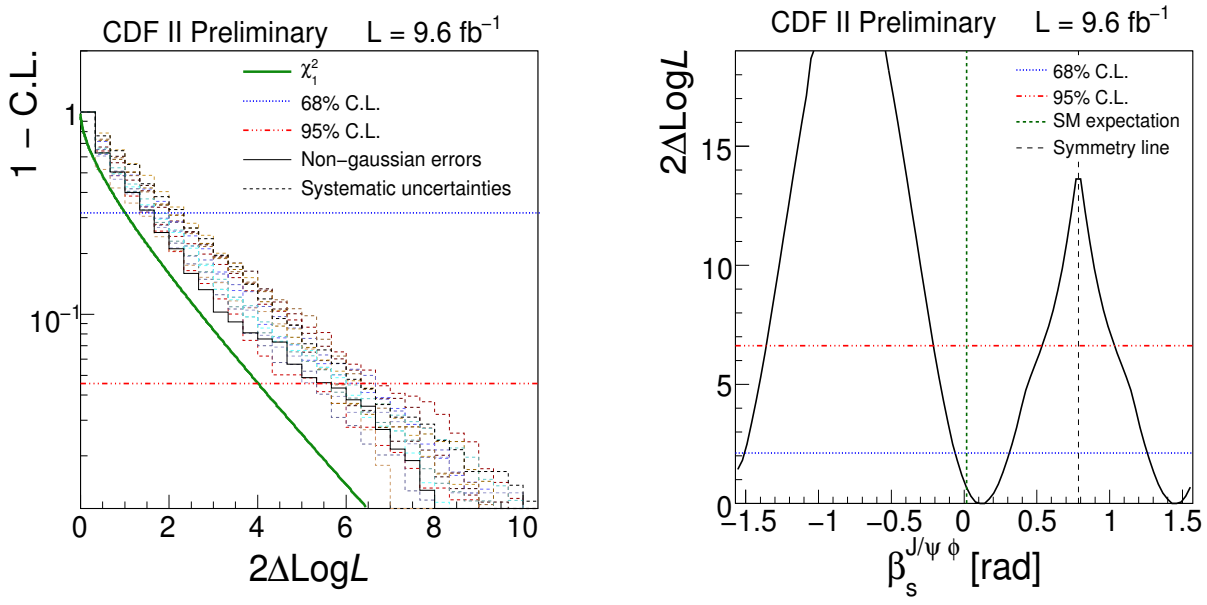

(a) (b)

Figure 8. Profile-likelihood ratio distribution with one degree of freedom ($\beta_s^{J/\psi\phi}$) observed in pseudo experiments mimicking our data (a) and corresponding confidence intervals (b) for $\beta_s^{J/\psi\phi}$.

Source	$c\tau(B_s^0)$ [μ m]	$\Delta\Gamma$ [ps $^{-1}$]	$\lvert A_\parallel(0)\rvert^2$	$\lvert A_0(0)\rvert^2$	$\delta_\perp$
Signal angular acceptance	0.29	0.0014	0.0134	0.0162	0.076
Signal mass model	0.17	0.0007	0.0006	0.0020	0.018
Bckg mass model	0.14	0.0006	0.0003	0.0002	0.034
Decay time resolution	0.52	0.0010	0.0004	0.0002	0.066
Bckg decay time model	1.31	0.0057	0.0006	0.0012	0.064
Bckg angular model	0.46	0.0037	0.0011	0.0022	0.009
Bias from mass uncertainty distribution	0.85	0.0006	0.0003	0.0002	0.036
Bias from decay time uncertainty distribution	0.63	0.0006	0.0003	0.0002	0.038
$B^0 \to J/\psi K^*$ cross-feed	0.18	0.0018	0.0002	0.0015	0.034
Vertex detector alignment	2.0	0.0004	0.0002	0.0001	0.034
Fitter bias	0.2	0.0012	0.0021	0.0008	0.02
Total	2.7	0.007	0.014	0.017	0.15

Table II. Summary of systematic uncertainties.

lifetime measurements, and propagated to all our results using pseudoexperiments. Table II lists the individual systematic uncertainties and the total one derived from adding in quadrature.

V. CONCLUSIONS

We reported an updated measurement of the *CP*–violating phase $\beta_s^{J/\psi\phi}$ using approximately 11 000 $B_s^0 \to J/\psi\phi$ decays reconstructed in 9.6 fb^{-1} of integrated luminosity collected by the dimuon trigger, which corresponds to the full CDF Run II dataset. The *CP*–violating phase is found to be $\beta_s^{J/\psi\phi} \in [-\pi/2, -1.51] \bigcup [-0.06, 0.30] \bigcup [1.26, \pi/2]$ ($[-\pi/2, -1.36] \bigcup [-0.21, 0.53] \bigcup [1.04, \pi/2]$) at the 68% (95%) CL, in agreement with the expectation from the CKM hierarchy. Assuming that value for $\beta_s^{J/\psi\phi}$ we also determine the mean B_s^0 lifetime, $\tau(B_s^0) = 1.528 \pm 0.019$ (stat) $\pm$ 0.009 (syst) ps; the width difference between heavy and light mass eigenstates, $\Delta\Gamma_s = 0.068 \pm 0.026$ (stat) ± 0.007 (syst) ps^{-1}; and the transversity amplitudes, $|A_0(0)|^2 = 0.512 \pm 0.012$ (stat) ± 0.017 (syst), $|A_\parallel(0)|^2 = 0.229 \pm 0.010$ (stat) $\pm$

0.014 (syst) and the strong phase $\delta_\perp = 2.79 \pm 0.53$ (stat) ± 0.15 (syst) rad. From these results we derive also the ratio $\frac{\Delta\Gamma_s}{\Gamma_s} = 0.1045 \pm 0.048$ (stat) ± 0.011 (syst) and, using the world average [4] B^0 lifetime , $\frac{\tau(B_s^0)}{\tau(B^0)} = 1.006 \pm 0.015$ (stat + syst), in agreement with theoretical expectations. All results are consistent with determinations from other experiments. They also agree and supersede previous CDF determinations.

VI. ACKNOWLEDGEMENTS

We thank the Fermilab staff and the technical staffs of the participating institutions for their vital contributions. This work was supported by the U.S. Department of Energy and National Science Foundation; the Italian Istituto Nazionale di Fisica Nucleare; the Ministry of Education, Culture, Sports, Science and Technology of Japan; the Natural Sciences and Engineering Research Council of Canada; the National Science Council of the Republic of China; the Swiss National Science Foundation; the A.P. Sloan Foundation; the Bundesministerium für Bildung und Forschung, Germany; the Korean World Class University Program, the National Research Foundation of Korea; the Science and Technology Facilities Council and the Royal Society, UK; the Russian Foundation for Basic Research; the Ministerio de Ciencia e Innovación, and Programa Consolider-Ingenio 2010, Spain; the Slovak R&D Agency; the Academy of Finland; and the Australian Research Council (ARC).

[1] T. Aaltonen *et al.* [CDF Collaboration], arXiv:1112.1726 [hep-ex].
[2] V. M. Abazov *et al.* [D0 Collaboration], Phys. Rev. D **84** (2011) 052007, arXiv:1106.6308 [hep-ex].
[3] D. Acosta *et al.* [CDF Collaboration], Phys. Rev. D **71** (2005) 032001.
[4] K. Nakamura *et al.* [Particle Data Group], J. Phys. **G 37** (2010) 075021 and 2011 partial update for the 2012 edition.
[5] J. Morlock, Ph. D. thesis, University of Karlsruhe, Report No. IEKP-KA/2010-13 (2010).
[6] V. M. Abazov *et al.* [D0 Collaboration], arXiv:1109.3166 [hep-ex].
[7] R. Aaij *et al.* [LHCb Collaboration], arXiv:1112.3183 [hep-ex].